COMPUTER ANALYSIS OF LARGE-SCALE STRUCTURES

ary of Congress Catalog Card Number 81-69006

FOREWORD

Computer analyses of large-scale structures are now common activities that cut across different disciplines such as civil, mechanical and aeronautical engineering. Most technical meetings on computational structural mechanics have been concerned with new methods such as finite elements, solution algorithms and computer implementation aspects. On the other hand, most user-oriented workshops have been concerned with what one can do with commercial structural analysis programs. The editors have come to believe that there exists a need to link the technical conferences to the program users and vice versa. This involves from the user's viewpoint, for example, how one arrives at the selections of discretization techniques, material characterizations and element sizing; how to discern the many exceptions and pitfalls of the methods selected for intellignet usage; and, how computer software advances impact the design of the structural analysis program. Of interest to the methods developer are the time delay from publication to actual implementation in production programs, the impact of budget and scheduling constraints on the modeling, the selection of specific programs and accuracy compromises, and the role of pre and post-processors as dominant concerns by many users (if it is not easy to use most users tend to shy away from that program!).

The six papers in this volume represent diverse problems in computer analyses of structural systems. With a few exceptions most authors in the volume fall in the category of intermediate users in that they develop for themselves a considerable part of the total required analysis software even though they utilize commercial programs. The editors therefore hope that this volume will contribute to bring the methods developers and the structural analysis program users closer together and thank the authors for their contributions.

K. C. Park
R. F. Jones, Jr.

CONTENTS

DYNAMIC ANALYSIS OF A HEMISPHERICAL CONTAINMENT STRUCTURE SUBJECTED TO TRANSIENT LOADS

A. D. Gupta and H. L. Wisniewski
Therminal Ballistics Division
US Army Ballistic Research Laboratory
Aberdeen Proving Ground, Maryland

ABSTRACT

Large deflection elastic-plastic response of a 9 m radius hemispherical shell enclosure structure .0254 m thick clamped to a horizontal rigid foundation subjected to explosive blast loading due to a 29.03 kg TNT charge at the center was analyzed using a finite-difference structural response code, i.e., PETROS 3.5.

The peak reflected overpressure was estimated from a scaled distance of the wall from the point of detonation based on a conservative cube-root scaling law. The reflected overpressure decay with time was assumed to obey the modified Friedlander equation. The residual quasi-static overpressure was obtained from an equation developed by Kinney and Sewell based on the ratio of the available vent area and the internal volume.

Only a quarter segment of the structure was modelled using 17 equal width meshes in one layer and four Gaussian integration points through the thickness in each mesh. The 1020 steel was represented by a trilinear curve followed by a perfectly-plastic behavior and elastic-plastic unloading resulting in a polygonal approximation.

The results indicated the initiation of flexural waves at the clamped edge propagating towards the pole and thereby altering the spherically symmetric breathing mode of response of the structure. The peak deflection was predicted by the code to occur at the pole and permanent displacement after releasing the load was found to be quite small. Transient strain components at the inner and outer surfaces near the clamped edge due to mainly elastic oscillations showed significant bending deformation. In conclusion, the protective structure was found to be efficient configuration capable of safe containment of internal explosive blast loading.

NOMENCLATURE

α - exponential decay parameter
ρ - density of material, kg/m^3
ν - Poisson's ratio
σ - meridional stress, kPa
σ_y - static yield stress, kPa
ϵ_y - yield strain in biaxial tension
A_v - available vent area, m^2
E - modulus of elasticity, MPa
K - empirical curve-fit constant = 4.08×10^{-6} m^3/kg

P_m - peak reflected overpressure, MPa

P_o - peak quasi-static pressure, MPa

P_r - reflected overpressure, MPa

R - mean radius of the hemisphere, m

T - time period of oscillation, ms

V - internal enclosure volume, m^3

W_E - equivalent charge weight of explosive, kg

Z - scaled distance of the wall from the charge location, $m/kg^{1/3}$

h - wall thickness, m

t_g - blow-down time, ms

t_o - positive phase duration of impulse, ms

INTRODUCTION

The Ballistic Research Laboratory is currently in the process of acquiring a target enclosure to facilitate destructive terminal ballistic testing of chemical explosives (CE), special armor and kinetic energy (KE) penetrators by safe containment of blast, fragments and resultant harmful combustion products. The present investigation is based on a preliminary concept of the firing range as shown in Figure 1. The target is located inside the hemispherical enclosure at the end of a long concrete pipe-guide. The gun-launched projectile travels through the pipe-guide and enters the enclosure through a .914 m diameter entrance hole. The target interaction with the projectile is monitored photographically with flash X-ray equipment and penetration velocity is obtained using velocity screens and electronic counters. An air exhaust system mounted at the rear of the structure operates during the test and draws back aerosolized material out of the enclosure after a test and traps it in filters in the exhaust ducting. A large sliding door with a configuration to match the curvature of the hemispherical wall allows equipment access inside the enclosure. The door is sealed to the wall with a pressurized hose seal along its perimeter. The entire structure is built to contain blast and fragments, to trap aerosolized materials and to permit photographic observation of the test.

A significant problem associated with the enclosed range tests is the overpressure resulting from shock loading as well as rapid heating of the air within the enclosure as the penetrator and the target are torn apart during their encounter as shown by R. Abrahams et al. [1]. The structure must survive both the reflected and the residual overpressures induced by the interaction until ambient conditions are reached due to venting out to the atmosphere through the exhaust system.

Since the key element of the AHKELS (Advanced High Kinetic Energy Launch System) range is the enclosure structure, the Target Loading and Response Branch was assigned to estimate the overpressure loading on the wall and analyze dynamic response of the preliminary configuration at critical locations and assure structural integrity from a conservative viewpoint. The choice of a hemispherical configuration was confirmed by an earlier investigation by N.J. Huffington et al. [2] who demonstrated the effectiveness of such a protective structure.

In the absence of any available experimental data it was decided to obtain a theoretical estimate of the transient and residual overpressure loading due to a centrally located equivalent charge weight at the base. The subsequent objective was to perform an approximate conservative static analysis for an initial estimate of wall thickness. Finally the dynamic elasto-plastic, large deflection response of the shell configuration clamped to a horizontal rigid foundation was studied to indicate critical locations where peak strains or deflections could occur.

ESTIMATION OF TRANSIENT LOADS

The transient loads were estimated under the assumption that the test firing of penetrator rounds would generate overpressures inside the containment chamber similar to those caused by an internal blast due to an equivalent central charge weight of 29.03 kg at the base as shown in Figure 2. Assuming the walls to be

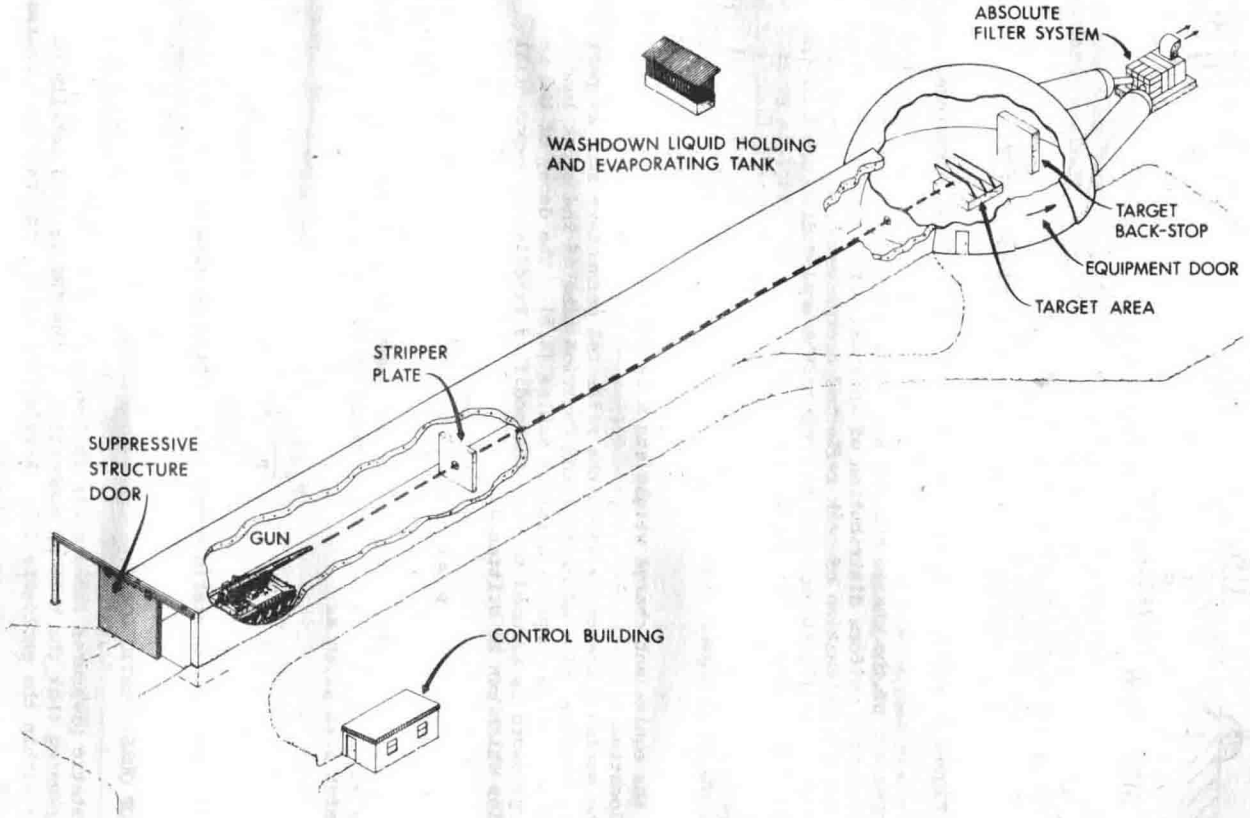

Figure 1 Preliminary concept layout of the AHKELS (Advanced High Kinetic Energy System) range

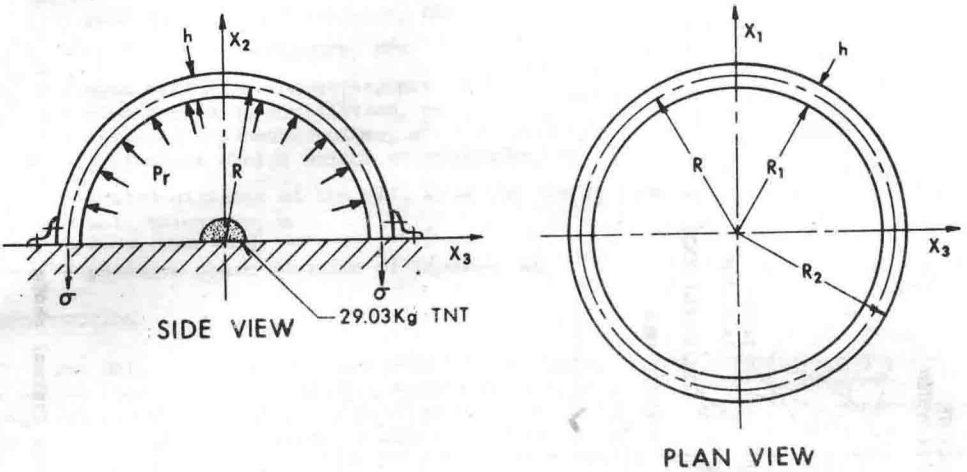

Figure 2 Section through hemispherical containment structure

rigid, the symmetry of the charge and the structure about a vertical axis through the center indicates uniform distribution of internal reflected loading upon the structure. For the estimation of peak reflected overpressure, a conservative cube-root scaling law [3] is employed to compute the scaled distance Z of the wall from the charge location in the form

$$Z = \frac{R}{W_E^{1/3}} \tag{1}$$

where W_E is the equivalent charge weight and R is the distance of the wall from the charge location.

Once the scaled distance is known the reflected parameters such as peak overpressure, impulse, time of arrival and duration time of the shock loading could be estimated from compiled airblast tables [4,5]. The decay of the reflected overpressure is assumed to obey the modified Friedlander exponential decay equation which can be written as

$$P_r = P_m[1 - t/t_o]e^{-\alpha t/t_o} \tag{2}$$

where t_o is the positive phase duration of the impulse, P_m is the peak reflected overpressure and t is the elapsed time from impact or detonation. The exponential decay parameter α is given as

$$\alpha = .57\left(\frac{P_m + P_o}{P_o}\right)^{0.65} \tag{3}$$

where P_o is the peak quasi-static overpressure obtained from residual overpressure calculations.

ESTIMATION OF QUASI-STATIC LOADS

Quasi-static pressures immediately following the reflected pressure were predicted assuming that the heat of combustion of the TNT is used totally to heat the air within the enclosure [6]. A relationship for the resultant increase in pressure is

$$\Delta P = \frac{0.4\ hW_E}{V}, \text{ kPa}, \tag{4}$$

where

$V = 1513.9\ m^3$, the internal volume of the enclosure
$W_E = 29.03$ kg, weight of the explosive charge
$h = 13.5$ KJ/g, the heat of combustion of TNT.

An internally pressurized structure vents the pressure to the surroundings through openings in its walls causing a slow decay to ambient condition as shown by Kinney and Sewell [7] and is computed from

$$\text{Ln } P = \text{Ln } P_o - .315\ (A_v/V)\ t\ , \tag{5}$$

where

t = elapsed time in ms
P = absolute pressure at t_s
$A_v = 2.33\ m^2$, the available vent area.

The long term duration of the decay is essentially due to the relatively small vent area available causing a slow pressure decay to the atmosphere.

The blow-down time t_s, required to reduce the residual overpressure to ambient conditions developed by Keenan et al. [8] based on the firing of high explosives in chambers with known vent areas and volumes is given as

$$t_s = 6.28\ (A_v/V)^{-.86} \tag{6}$$

The above equation is valid for $A_v/V^{2/3} < 0.21$. In the current design the ratio $A_v/V^{2/3}$ equals .018 and the duration time for the quasi-steady pressure is approximately 1600 ms.

The computation involves determination of peak residual overpressure from Eq. (4) which when combined with Eqs. (5) and (6) yields the quasi-steady part of the loading history. The junction between the reflected overpressure history and the quasi-steady loading is smoothed by a curve interpolation scheme in order to avoid a sharp transition. The resulting load profile is shown in Figure 3. This loading is applied uniformly at each meshpoint on the inside

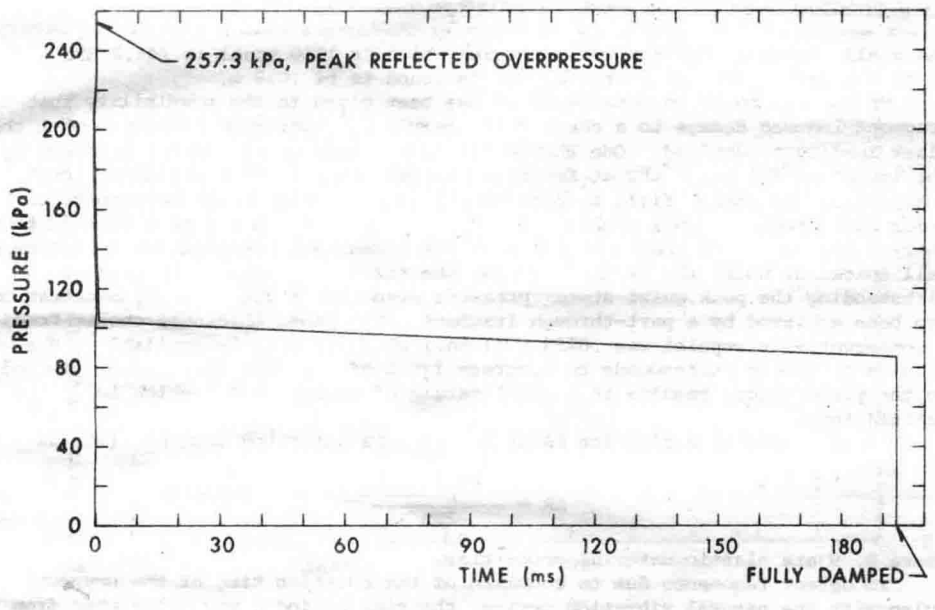

Figure 3 Computed pressure-time history due to internal explosive blast loading of the hemispherical enclosure

wall in the radial direction in the finite-difference structural response model in the PETROS 3.5 computer program [9]. In Figure 3 the load-time history inside the hemispherical enclosure was zeroed out after 180 ms to facilitate damping of small elastic oscillations and to observe any residual deformation of the hemispheric wall. The peak reflected overpressure was found to be 257.3 kPa while the peak residual overpressure was approximately 100 kPa.

STATIC STRESS ANALYSIS

Prior to a detailed dynamic response study, a static stress analysis in the linear-elastic-small deflection regime was conducted to obtain an initial estimate of the enclosure wall thickness. Since the duration of the reflected pressure is less than 1.5 ms compared to 1600 ms for the duration of the quasi-steady overpressure, an approximate static analysis, based on a minimum factor of safety of 2.0 is considered to be satisfactory. For the preliminary investigation, stress-concentration near holes, cutouts and wall openings was neglected. However the effect of ground-plane reflection of the shock wave was included through a load multiplication factor of $k = 2.0$, which in effect doubled the applied load.

To contain the initial pressure pulse in an elastic manner only the peak reflected overpressure P_r was included in the calculation of stresses and deflections. An equivalent static meridional stress σ can be calculated from Figure 2 by equating the resultant upward force due to internal pressurization to the net downward restraining force due to the stress developed at the clamped edge resulting in

$$\sigma = \frac{RkP_r}{2h} \tag{7}$$

where

R = 8.987 m, the median radius
k = load multiplication factor.

However for an assumed factor of safety of 2.0 $\sigma = 1/2\ \sigma_y$, where σ_y is the static yield stress. Substituting this value of σ in Eq. (7) and rearranging terms results in an expression for the estimated thickness h in the form

$$h = \frac{RkP_r}{\sigma_y} \tag{8}$$

The yield stress σ_y for the wall material which is 1020 steel is 241.3 MPa. Hence the wall thickness h from Eq. (8) is found to be .019 m.

Up to this point no consideration has been given to the possibility that fragment induced damage to a shell might result in catastrophic rupture when the blast loading is applied. One should estimate the material removal produced by the impact of the worst threat fragment and perform a local three-dimensional analysis of the stress field to determine whether a crack would be propagated under such loading. This problem in fracture mechanics is rather difficult to analyze and can be at least partially circumvented by a conservative selection of wall thickness under the assumption that the residual thickness is capable of withstanding the peak quasi-steady pressure even when a 50% depth of penetration has been achieved by a part-through fragment. The final thickness chosen from a conservative viewpoint was .0254 m (1 in.) which is readily available. The .0254 m thickness corresponds to a stress level of 45.5 MPa which when compared to the yield stress results in a final margin of safety of 4.3 which is satisfactory.

The peak radial deflection ΔR at the pole is estimated from Ref. [10] as

$$\Delta R = \frac{R^2 kP_r (1 - \nu)}{2Eh} \tag{9}$$

where E, ν are elastic material properties.

To detect resonance due to coupling of the duration time of the pressure pulse with the natural vibration period, the time period T was calculated from Ref. [10] as

$$T = \pi R \sqrt{\frac{2\rho (1 - \nu)}{E}} \tag{10}$$

where ρ is the mass density. Further check of any interaction of the reflected pressure pulse due to ground plane reflection with the elastic oscillation of the pole did not reveal a significant problem.

The peak radial elastic deflection at the pole from Eq. (9) was found to be .0011 m which is quite small. The gross weight of the hemispherical enclosure was found to be approximately 96,400 kg based on an .0254 m wall thickness. In this study allowance was made for the weight of flanged material at the base but not for extra weight associated with access provisions, welds or foundations.

An optimization study based on equivalent strength showed substantial weight saving for a hemispherical configuration at or below 6 m radius but marginal savings at higher radius up to 9 m due to compensating thickness increases. An equation proposed by R. Karpp et al. [11] for the minimum amount of vessel material V_m to contain a specified charge is given as

$$V_m = 4\pi M \left(\frac{k}{\varepsilon_y}\right)^{1.0406} \rho^{.0406} \left(\frac{R}{h}\right)^{.0406} \qquad (11)$$

where ε_y is the yield point strain of the vessel material in biaxial tension, M is the charge weight, ρ is the density of the vessel material and k is an empirical curve-fit constant found to be 4.08×10^{-6} m^3/kg. Unfortunately the optimum configuration could not be achieved due to constraints of minimum workspace and equipment access requirements.

DYNAMIC RESPONSE ANALYSIS

Response of the structure subjected to transient loads from an instant blast shown in Figure 2 was conducted using the BRL version of the PETROS 3.5 computer program [9], which employs the finite-difference method to solve the nonlinear equations governing finite-amplitude elastoplastic response of thin Kirchhoff shells. The model is valid for large deflections and can be employed to treat the entire structure rather than a small section.

Material Model

The uniaxial tensile quasi-static stress-strain property for 1020 steel which is used as the primary vessel material is shown by the continuous line in Figure 4. The material is modelled in the code as a combination of three linear

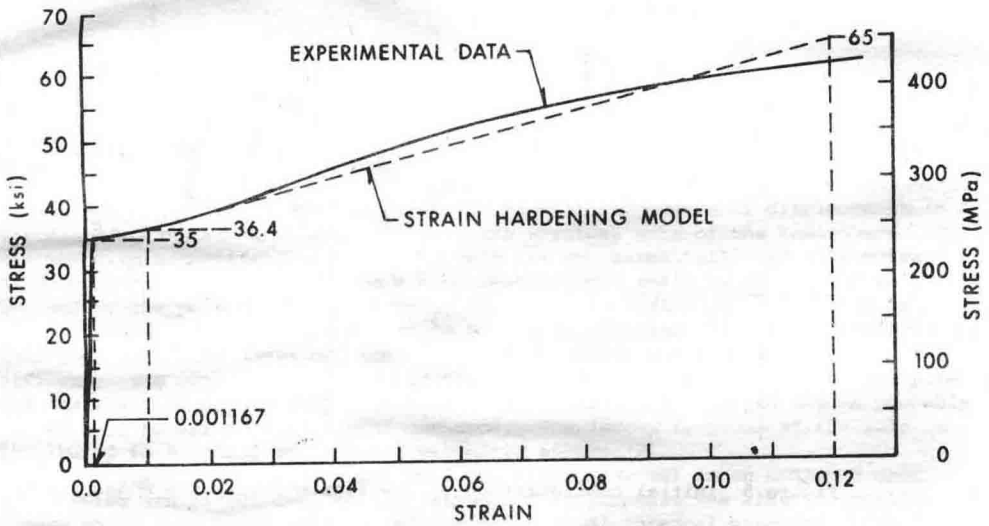

Figure 4 Stress-strain property modelling

segments indicated as the dashed curve in Figure 4, followed by perfectly-plastic behavior and linear elastic-plastic unloading, resulting in a polygonal approximation of the experimental data. The strain-hardening part of the stress-strain curve is generated by a sublayer hardening model from a weighted combination of elastic perfectly-plastic curves yielding a piecewise multilinear hardening representation. Strain-rate effects were neglected, which is conservative since these effects increase the structural resistance and thus reduce the total deformation.

Finite-Difference Model

Since both the responding structure and the applied loads are symmetric with respect to the vertical axis as shown earlier in Figure 3, it is sufficient to model the response of a single pie-shaped segment of the hemispherical enclosure and generate the entire structure by 360° rotation of the structure about the axis of symmetry resulting in quite economical computer runs.

A total of 18 meshes along the surface and a single layer through the thickness were used to represent the pie-shaped segment. Four Gaussian integration points through the thickness were used at each mesh for computational purpose. The total number of mesh points did not exceed 37. Initial configuration of the finite-difference model employed for all subsequent calculations is shown in Figure 5.

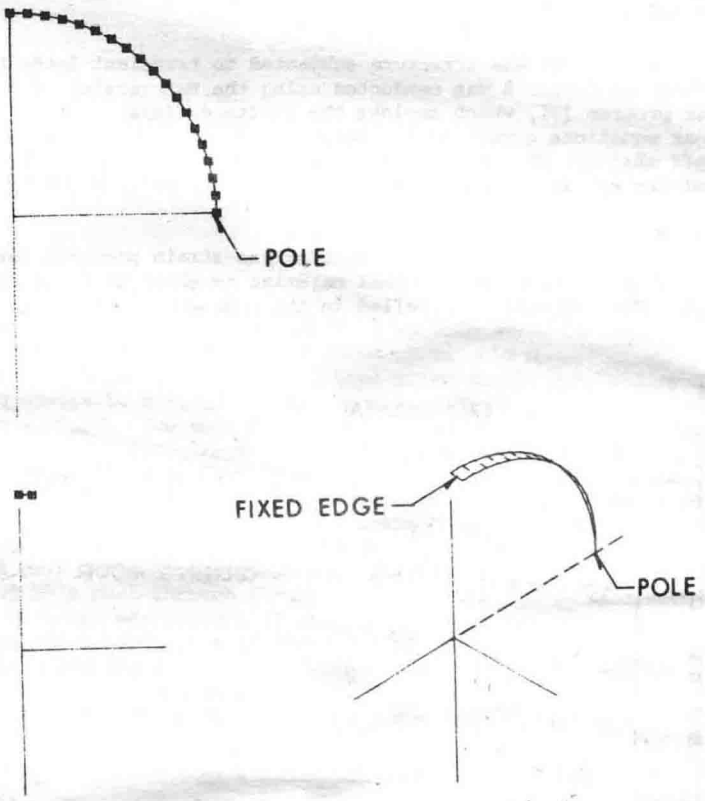

Figure 5 Initial configuration of the finite-difference model

RESULTS AND DISCUSSION

The deformed cross-section of the hemispherical segment is shown in Figure 6 relative to the initial undeformed configuration at 36 ms which is approximately the time at which maximum deflection occurs at the pole. The deflections are exaggerated due to a high magnification factor of 1000 and are, in fact, small enough to be in the linear elastic range.

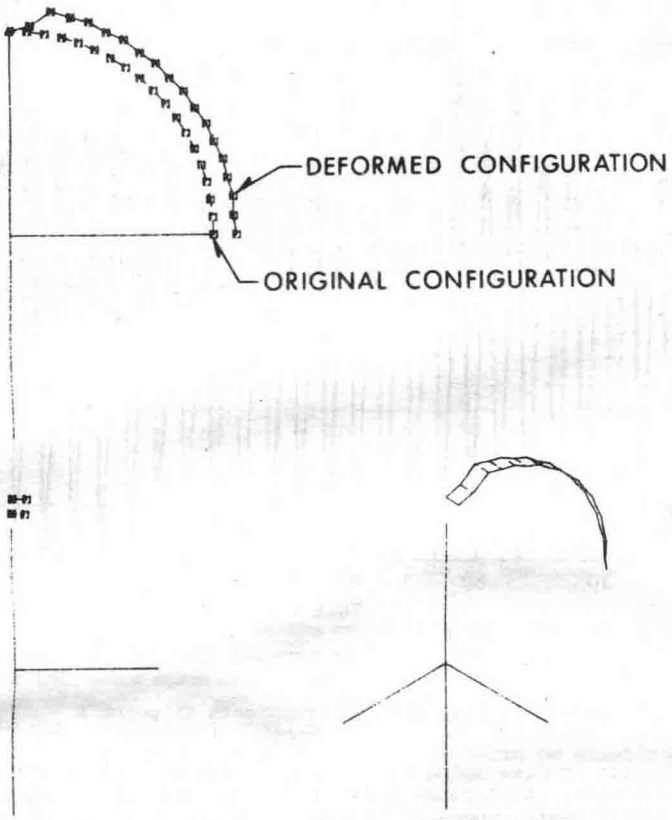

Figure 6 Deformed configuration at 36 ms corresponding to cycle No.1500

Figure 7 describes the transient rectangular components of displacement in a meridional plane at point A at 45° from the vertical axis of the hemisphere. The maximum displacement at this point is only .82 mm, essentially radially outward. Displacements at other locations are correspondingly small except in the neighborhood of the pole of the hemisphere, where a peak deflection of 1.17 mm is observed after 30 ms as illustrated in Figure 8. However this displacement is less than 4% of the shell thickness so that geometric nonlinearities are insignificant. The peak deflection is of the order of elastic deflection at the pole and any residual deflection after elastic oscillations are damped out is probably caused by a numerical artifact of the code. The larger response at the pole is attributed to focusing of flexural vibratory energy [2].

The PETROS 3.5 code was run for 8000 cycles (192 ms) in an undamped mode, after which artificial damping was introduced to suppress the elastic oscillations, which were positively biased due to residual internal pressure. Damping was facilitated by zeroing out the internal pressure. Fully damped condition was achieved at cycle 8235 (198 ms) when the final configuration was found to be

identical to the undeformed configuration in Figure 5 with no evidence of plastic deformation.

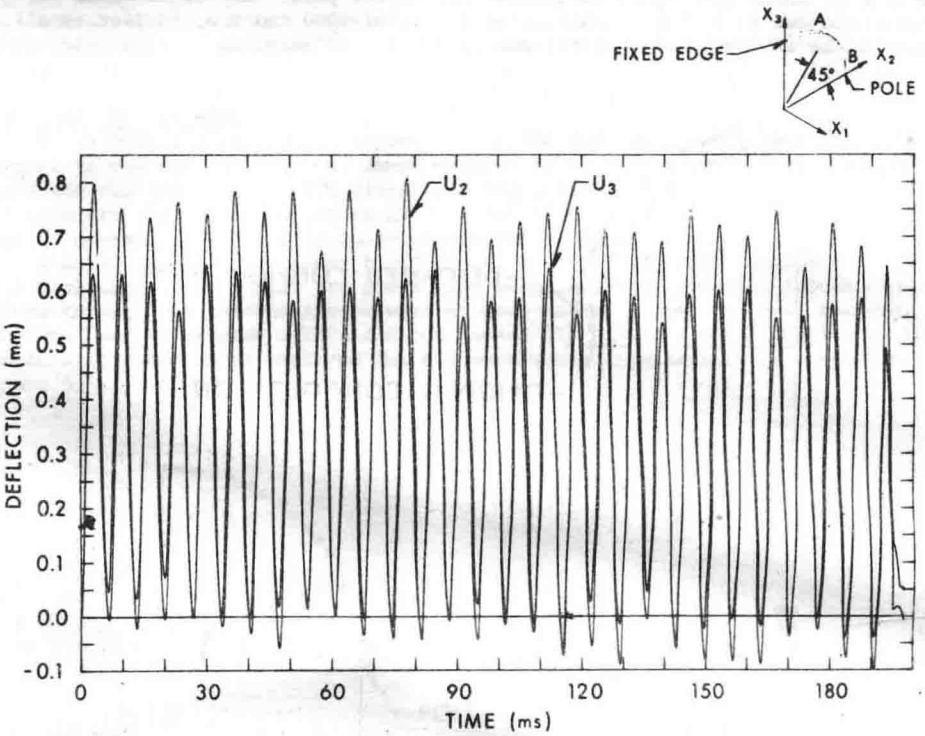

Figure 7 Transient displacement components at point A

Energy balance studies using the code confirmed absence of plastic work and numerical instability. Both total and kinetic energies were bounded. The fluctuations of kinetic energy appeared to have twice the frequency of the work performed by the internal blast pressure.

Transient strain components on the outer and inner surfaces of the hemisphere at a point near the edge are shown in Figures 9a and 9b, respectively. The meridional strain components on the inner and outer surfaces are almost in phase initially but become out of phase and unequal in magnitude with increasing time signaling the build-up of some flexural deformation. The hemisphere moves outward and inward, except at the fixed boundary in a breathing mode resulting in membrane strains upon which the bending strains are subsequently superposed due to propagation of flexural waves from the fixed boundary towards the pole. Significant difference in strains between the outer and the inner walls at the clamped edge could be primarily attributed to domination of the response by the bending strains. The circumferential strains indicated by continuous lines in Figures 9a and 9b are zero as expected. Calculations for maximum meridional stress based on peak strain results in a stress level of 48.26 MPa which is equivalent to a safety margin of 4.0. As expected from elastic theory peak strains occurred at the fixed edge while maximum deflection occurred at the pole.

The variation of strain at the inner wall with time at a point near the pole is shown in Figure 10. The continuous line depicts the circumferential strain which is in phase and very similar to the meridional strain shown by the

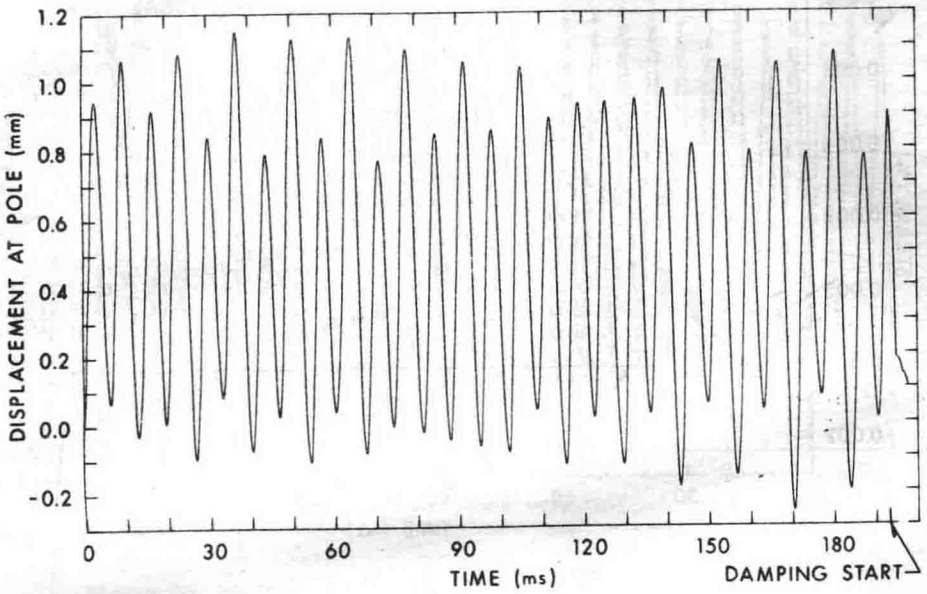

Figure 8 Transient displacement at pole of hemisphere

intermittent line. The strains at the outer wall near the pole exhibit elastic oscillations of approximately the same magnitude and duration as in Figure 10. This behavior indicates substantial weakening of the flexural wave near the pole and domination of meridional and circumferential strains by the membrane component of strain due to elastic vibration of the wall in the breathing mode. The peak meridional stress at the pole was calculated based on elastic equations and was approximately 25 MPa, which is considerably lower than the maximum stress at the clamped edge. The stress level is equivalent to a safety margin of 3.6 based on the yield stress.

Both strain components are relieved completely upon damping at approximately 198 ms. An isometric view of the fully damped configuration generated by 360° rotation of the pie-shaped segment about the axis of symmetry is shown in Figure 11. The view through section A-A shows the final configuration upon damping superposed on the initial configuration. The coincidence of the two configurations at a high magnification ratio of 1000 indicates the absence of any plastic deformation and confirms small strains and deformations throughout the structure in accordance with earlier results.

CONCLUDING REMARKS

It has been demonstrated, through use of a rigorous nonlinear shell response methodology, that it is possible to design a containment structure with a hemispherical configuration in an efficient and cost effective manner. The methodology could be easily extended to structural optimization studies, resulting in considerable cost savings, provided internal volume and access considerations could be met.

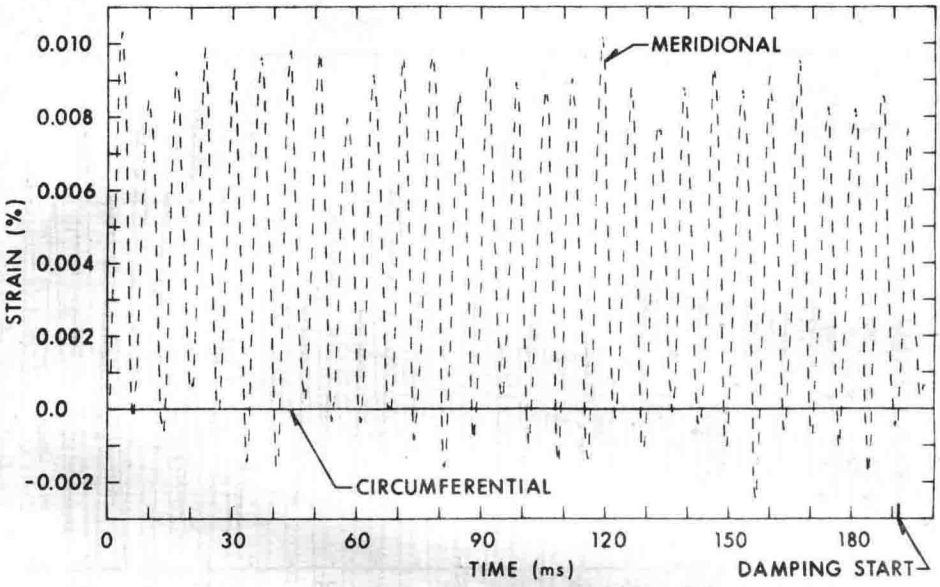

a) Outer surface strain components

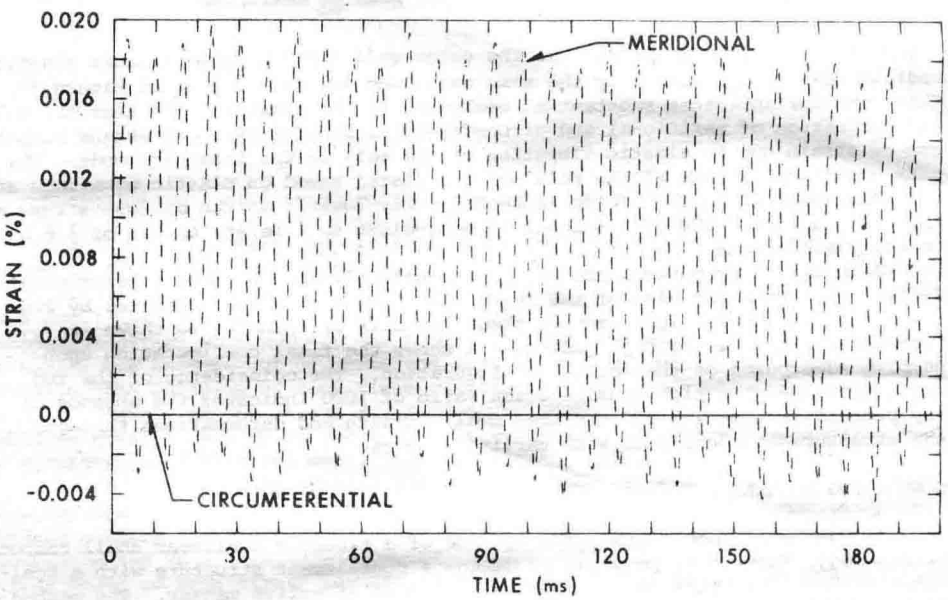

b) Inner surface strain components

Figure 9 Surface strains at the fixed edge

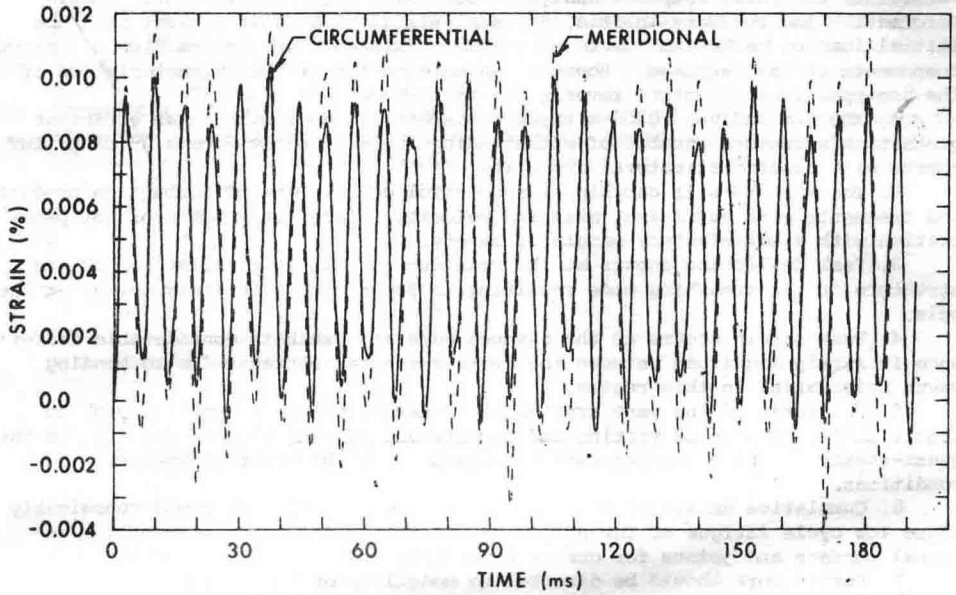

Figure 10 Surface strains at the inner wall near pole

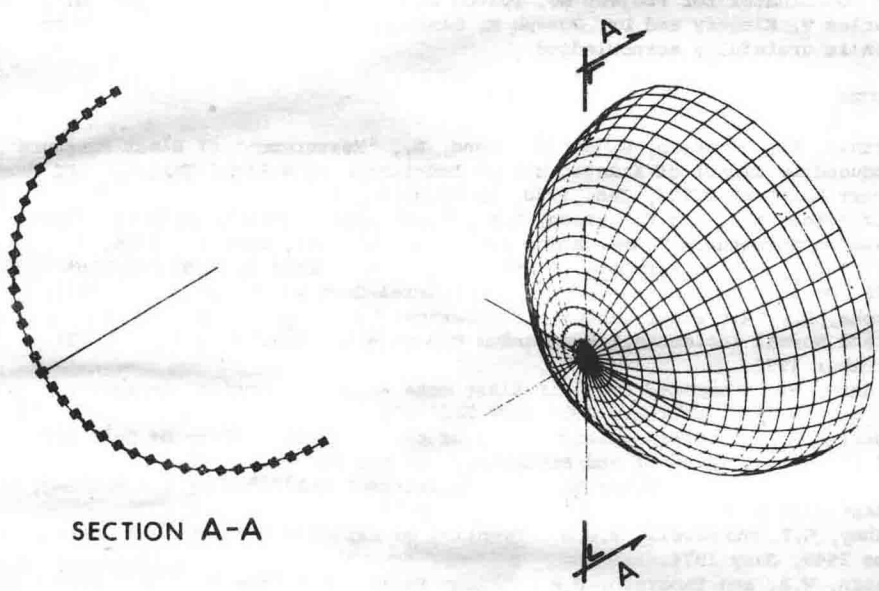

Figure 11 Isometric and sectional view of the fully damped configuration